Push-Up Load Tests Using Uncrushable Particles And Its Dem Analyses

SuriyahThongmunee[1], Shun-ichi Kobayashi[2] and Tatsunori Matsumoto[2]
[1]*Doctoral Student, Graduate School of Natural Science and Technology, Kanazawa University, Kanazawa, Japan*
[2]*Graduate School of Natural Science and Technology, Kanazawa University, Kanazawa, Japan*
Corresponding Author, E-mail: suriyah@stu.kanazawa-u.ac.jp, thongmunee@hotmail.com

ABSTRACT: In this study, push-up load tests of soil plugs having various aspect ratios in a steel pipe pile and its DEM analyses were carried out. Uncrushable uniform spherical particles (alumina balls) were used to model soil plugs. In order to obtain physical properties of the alumina ball, element tests of alumina balls, including one-dimensional compression tests and direct shear tests, shear tests between the model soil and the model pile and so on, were carried out. Then, DEM analyses of the one-dimensional compression tests and direct shear tests were carried out by matching the DEM results with the results of the element tests to obtain the analysis parameters to be used in DEM simulations of the push-up load tests. Thereafter, the push-up load tests and its DEM simulations were carried out. The results showed that the maximum push-up force increases with increase in aspect ratio and that hardening and softening behaviour of the push-up force occurs. These behaviours were totally in accordance with the experimental results. Finally, the experimental results in this paper are compared with the push-up load tests of the crushable sand plugs obtained in previous study, in which the push-up force increased monotonically with increasing push-up displacement. Possible influence of crushability of particles on the plugging behaviour during push-up loading is discussed, based on the comparison.

Keywords: Push-up load test, Uncrushable spherical particle, Crushable particle, Plugging behaviour, 3D-Discrete Element Method

1. INTRODUCTION

Open-ended pipe piles are widely used in many countries for foundation both on land and offshore. During driving process an open-ended pipe pile into the soil, a soil column is created inside the pile, which is well known as the soil plug. Depending on the relative motion between the pile and soil plug, the pile is said to be plugged, partially plugged or unplugged pile. If the pile is completely plugged, the soil plug moves downward together with the pile. Vice versa, in completely unplugging, the soil plug does not move downward with the pile. In partially plugging, the soil plug moves relative to the pile, so the height of the soil plug inside the pile is some fraction of the total embedded pile length.

Many researchers have investigated the plugging behaviour and mechanism of open-ended pipe piles. Plugging behaviour in fully-drained condition has been theoretically investigated by Yamahara 1964a, 1964b), and experimentally by Kishida and Isemoto (1977), Kanno et al. (1978), Hight et al (1996), de Nicola and Randolph (1997), Gavin and Lehane (2003), Paik and Salgado (2003), Kitiyodom et al (2004) and so on. Behaviours of open-ended steel pipe piles and soil plugs during driving and static loading were investigated in field conditions (e.g. Pawkowski and Whitman, 1990; Matsumoto and Takei, 1991; Byrne, 1995; Matsumoto et al., 1995; Paik et al, 2003). Numerical studies also have been conducted by Kishida and Isemoto (1977), Leong and Randolph (1991), Randolph et al. (1991), Randolph et al. (1992) and Liyanapathirana et al. (1998, 2000, and 2001). These researches showed that plugging behaviour depends on 4 parameters such as aspect ratio of soil plug, coefficient of friction between the pile and the soil, relative density of soil plug and drain condition of soil plug as well as loading rate.

Thongmunee et al (2010) carried out experimental and numerical studies on push-up loading of medium sand plugs in an open-ended steel pipe pile with different aspect ratios of sand plug, H/D. It was found that push-up force increases exponentially with increase in H/D. In the numerical study, 3D-Discrete Element Method (DEM) was employed. The DEM analyses of the push-up load tests showed good agreement with the test results well as long as crushing of sand particles did not occur. It was suggested that crushing of soil particles also has a significant influence on soil plug behaviour.

However, in case that crushed sand particle pieces are tiny and can migrate through the pore spaces between surrounding particles, it is thought that there is no influence of particle crushing on plugging behaviour. So, it is questionable that how the overall behaviour of soil plugs is influenced by particle crushing.

In this paper, push-up load tests of soil plugs and its DEM simulations were carried out with no influence of particle crushing. That is, uncrushable uniform spherical particles (alumina balls) were used to model soil plugs. Prior to the push-up load tests, element tests of the model soils, such as one-dimensional compression tests, direct shear tests of the alumina balls, shear tests between the model soil and pile and so on, and its DEM were conducted to characterise the alumina ball and to determine suitable analysis parameters to be used in DEM analyses of push-up load tests of plugs.

Moreover, the test results of push-up load tests of uncrushable soil plugs were compared with those of the crushable sand plugs which have been carried out by the authors, and discussion was made in term of possible influence of crushability of particles on the plugging behaviour.

2. INVESTICATION OF MODEL SOIL PROPERTIES

Uniform spherical alumina balls having 4 mm in diameter were used as uncrushable soil particles in this study. The alumina balls (Al_2O_3: 93%, SiO_2: 5%) are hard and brittle material with a fracture toughness of 3.2 MPa-$m^{0.5}$.

Although the diameter of 4 mm of the alumina balls seems to be relatively large compared to the inner pile diameter of about 100 mm, it was decided to use the alumina balls from the following reasons. An objective in this paper is to obtain insight to the behaviour of uncrushable soil plugs in an open-ended pipe pile through the comparison between the push-up load tests and their DEM analyses. Due to the limitation of calculation capacity of DEM analyses, the diameter greater of 4 mm was adequate. Another reason was based on the experimental results by Ovesen (1979). Ovesen (1979) carried out a series of centrifuge modelling of vertical load tests of rigid plates on the surface of a model ground of dry sand, in which centrifugal acceleration and plate diameter were varied to obtain the same proto type scale. The test results showed that if the plate diameter is greater and about 20 times the sand particle diameter, relative size of the sand particle and the plate diameter has little influence on overall (macro-scopic) behaviours of the plate and the ground. Referring to this result, the alumina balls 4 mm in diameter are thought be acceptable, because the ratio of the inner pile diameter to the ball diameter is around 25.

Prior to carry out the push-up load tests of soil plugs, element tests of the alumina ball and its DEM analyses were performed in

order to characterise the alumina balls and to determine suitable DEM analysis parameters.

The element tests included particle density test, maximum and minimum dry density tests, one-dimensional compression tests, direct shear tests of the alumina balls, shear tests between the alumina balls and the model pile, and friction tests between the alumina plates. DEM analyses of one-dimensional compression tests and the direct shear tests were carried out to determine suitable DEM analysis parameters.

2.1 Element Test of Alumina Balls

The results of the element tests are summarised in Table 1.

Particle density test, maximum and minimum dry density tests of the alumina balls were performed following the standard methods by Japanese Geotechnical Society (1992).

One-dimensional compression tests of the alumina balls were carried out using a special cylindrical box with an inner diameter of 60 mm and a height of 35 mm. The initial void ratio prior to applying vertical stress was set at 0.725 (relative density greater than 90%).

Direct shear tests of the alumina balls were carried out with 4 different normal stresses. The dimension of soil specimen after applying the normal stress was set at 35 mm in height and 60 mm in diameter. The initial void ratio prior to applying horizontal displacement was set at around 0.725.

The detailed results of both one-dimensional compression tests and direct shear tests will be shown later comparing with its DEM analyses.

Table 1 Physical and mechanical properties of the alumina ball

Property	Value
Diameter of alumina ball	4 mm
Density of soil particle, ρ_s	3.68t/m^3
Internal friction coefficient (friction angle) at peak, ϕ_p	0.72 (35.8 deg.)
Internal friction coefficient (friction angle) at rest state, ϕ_r	0.51 (26.9 deg.)
Maximum density, ρ_{max}	2.136 t/m^3
Minimum density, ρ_{min}	2.053 t/m^3
Maximum void ratio, e_{max}	0.792
Minimum void ratio, e_{min}	0.723
Fracture toughness, K_{Ic}	3.2 MPa-m$^{0.5}$

2.2 Shear Tests between Alumina Balls and Inner Pile Shaft Surface

The shear tests between the alumina balls and inner pile shaft surface of the model pile were performed to obtain the friction coefficient between them with condition that no rotation of balls was allowed, to estimate the interface friction coefficient to be used in DEM analyses.

The test set-up is shown in Fig. 1. The plastic bottle, with alumina balls glued on its surface and the lead balls inside it, was placed inside the model pile. Then, the bottle was pulled out using a winch and wire. The tests were carried out with 5 different weights of the plastic bottle, N, of 9.81, 19.62, 29.43, 39.24 and 49.05 N by changing the weight of lead balls inside the bottle. For accuracy, 4 tests were conducted in each weight. Throughout the tests, the friction force, F_{fric}, and the horizontal displacement were measured. The coefficient friction, μ, was calculated by the well-known formula ($\mu = F_{fric}/N$).

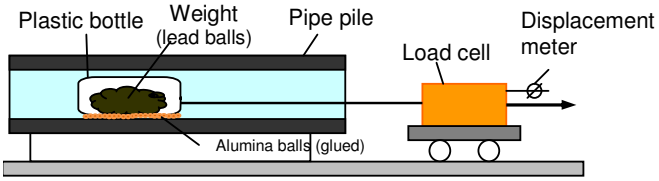

Figure 1 Illustration of device for direct shear test between the alumina balls and inner surface of the pipe pile (not to scale)

Figure 2 shows the results of the shear tests in case of a weight of 39.24 N. The results from 4 tests were very similar and the average interface friction coefficient between the alumina ball and the inner pile shaft surface was obtained as about 0.35 (friction angle = 19.3 deg.). Similar values were obtained also in the tests with other weights.

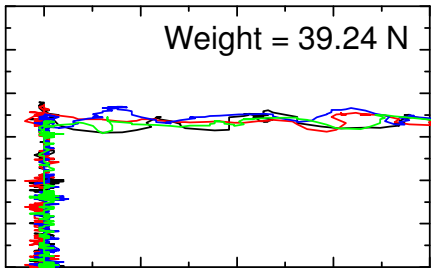

Figure 2 Example of results of shear tests between the sand and inner surface of the pipe pile

The properties of the model pile are summarised in Table 2. The inner pile diameter and the friction coefficient will be used in DEM simulations of push-up load tests of the uncrushable soil plugs.

Table 2 Properties of the model pipe pile

Property	Value
Young's modulus	201 GPa
Length	1.1 m
Inner diameter	93.2 mm
Outer diameter	101.4 mm
Friction coefficient (friction angle) between inner pile shaft and alumina ball	0.35 (19.3 deg.)

2.3 Friction Tests between Alumina Plates, and between Alumina Ball and Alumina Plate

Two series of friction tests including between two alumina plates and between the alumina ball and the alumina plate were carried out using an inclined plane method in order to estimate the friction coefficient between them.

Figure 3 shows an illustration of the friction test device used. The test device comprises a wood board, a weight, a lower alumina plate and an upper alumina plate without or with alumina balls adhered on its surface. The lower alumina plate was adhered to the wood board throughout the tests. Different weights, W, were placed on the upper alumina plate.

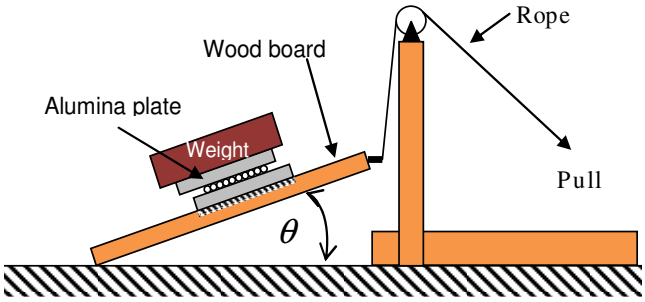

Figure 3 Illustration of inclined plane friction test device

First, the wood board with the lower alumina plate was set in horizontal plane. Then, the upper alumina plate without or with alumina balls was placed together with the weight on the lower alumina plate. Next, the wood plate was inclined by pulling the rope. The test was stopped when the upper plate started to move, and inclined angle of the wood board, θ, was measured. A total of 10 tests were carried out in each weight. Normal force, N, and friction force, F_{fric}, in each test were calculated from $W\cos\theta$ and $W\sin\theta$, respectively.

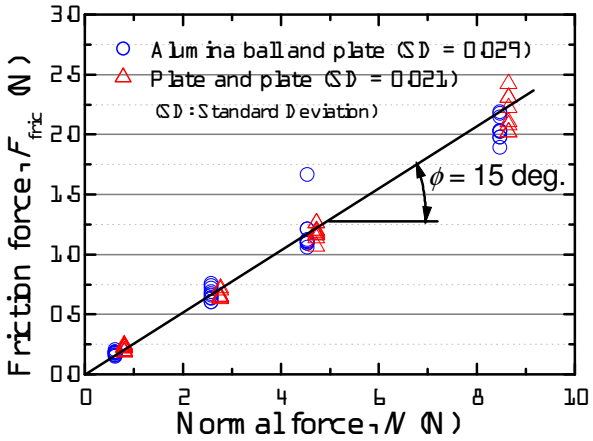

Figure 4 Relationship between normal force and shear force obtained in the friction test

Figure 4 shows the measured relationship between normal force and friction force. The friction forces were very similar in each given normal force. The average friction angle between two alumina plates and between the alumina ball and the alumina plate was obtained as 15 degrees that corresponded to 0.268 in friction coefficient. This value also will be used in DEM analyses of the element tests and the push-up load tests as a friction coefficient between alumina balls.

3. DETERMINATION OF ANALYSIS PARAMETERS

Discrete Element Method (DEM) was employed to simulate the push-up load tests in this study, because DEM is capable of calculating large deformations. The DEM code used in this study was PFC3D (Itasca, 2003).The alumina balls were modelled by rigid spherical particles.

3D-DEM analyses of the element tests including the one-dimensional compression tests and the direct shear tests of the alumina balls were carried out, in order to determine appropriate analysis parameters, such as normal and tangential spring stiffness between the spherical particles, by matching analysis between the element test results and its DEM simulations.

3.1 DEM Simulations of One-dimensional Compression Tests

DEM simulations of one-dimensional compression tests of the alumina balls in dense state were carried out. The normal spring stiffness was varied from 10^6 to 10^8 N/m. The ratio between tangential spring stiffness to normal spring stiffness was set at 1/4. Table 3 shows the analyses parameters of the spherical particles used in these DEM simulations.

Table 3 Analysis parameters and properties of spherical particles used in DEM of element tests

Property	**value**
Diameter of ball	4.0 mm
Density of ball particles, ρ_s	3.68 t/m^3
Friction coefficient (friction angle) between balls	0.268 (15 deg.)
Normal spring stiffness, k_n	10^6 to 10^8N/m
Tangential spring stiffness, k_s	k_n /4

Figure 5 shows analysis model of one-dimensional compression tests used in DEM. The one-dimensional compression box was modelled by rigid walls without consideration of side friction. The initial void ratio prior to compression was set at 0.730.

In the process of DEM analysis of the one-dimensional compression test, the spherical particles were generated inside the model of one-dimensional compression box. Then, a total of 8 loading steps starting from 9.81 to 1255.68 kPa were applied to the top of the specimen through the top rigid plate.

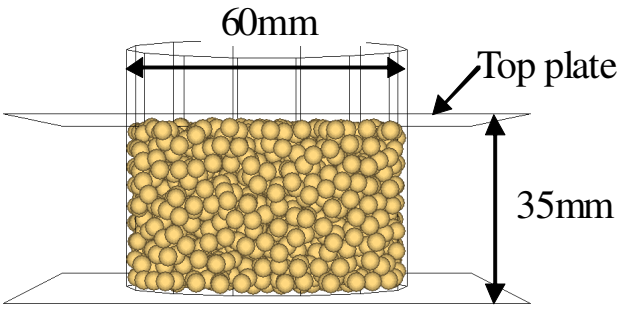

Figure 5 Analysis model of one-dimensional compression tests

Figure 6 shows comparison of the decrease in void ratio obtained from one-dimensional compression tests compared with its DEM results. Figure 6 indicates that the DEM simulations with low spring stiffness showed large decreasing rate of void ratio compared with the DEM simulations with high spring stiffness. The DEM analyses with k_n = ×10^6 N/m = 4k_s showed good agreement with the experimental results quantitatively.

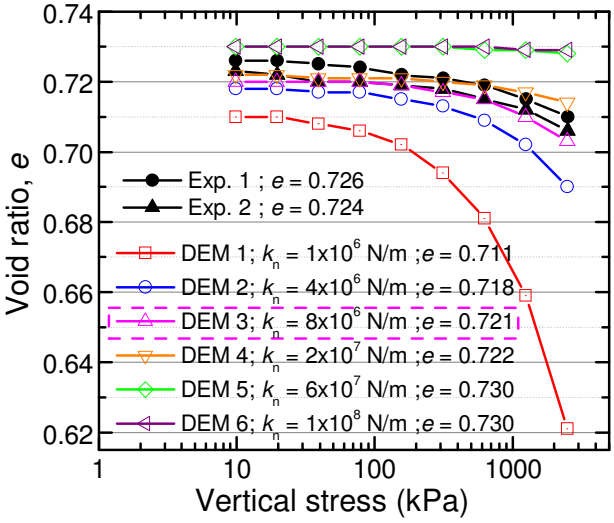

Figure 6 Comparison of changing of void ratio between one-dimensional compression test results and its DEM results

3.2 DEM Simulations of Direct Shear Tests

DEM simulations of direct shear tests (DST) of the alumina balls were also carried out for 4 different normal stresses, 19.62, 39.24, 78.48 and 156.96 kPa, using $k_n = 8\times10^6$ N/m = $4k_s$. The analysis model of the direct shear tests is shown in Fig. 7.

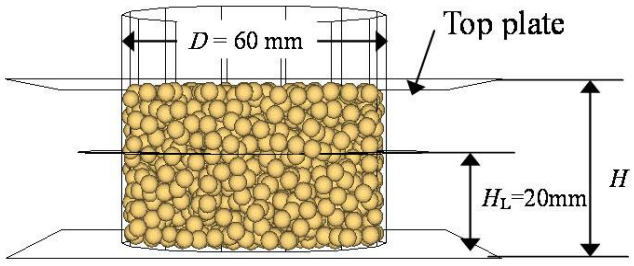

Figure 7 Analysis model of DSTs of alumina balls in DEM

In DEM analyses, the spherical particles were generated randomly inside the model shear box. Then, normal stress was applied to the top plate. After the completion the vertical loading stage, the horizontal displacement was applied to the upper part of the model shear box with a displacement rate of 0.4 mm/min.

The initial void ratio prior to shearing in each normal stress was almost equal to the value in the experiment.

Figure 8 shows comparison between the experimental results and its DEM simulation in case of 156.96 kPa in normal stress. The DEM analysis could simulate the shear stress well until the shear displacement up to 1 mm. After the shear displacement exceeded 1 mm, the DEM analysis tended to underestimate the experimental result although the DEM simulated the residual stress in the experiment well. This may be due to that the plane of loading plate (top plate) in DEM was kept perfectly in horizontal whereas the loading plate in the experiment could not be maintained in horizontal.

As for dilatancy behaviour (vertical strain), the DEM analysis simulated the vertical strain in the experiment well, although the DEM tended to overestimate the dilatancy in the experiment slightly. Similar results were observed in the other DEM simulations.

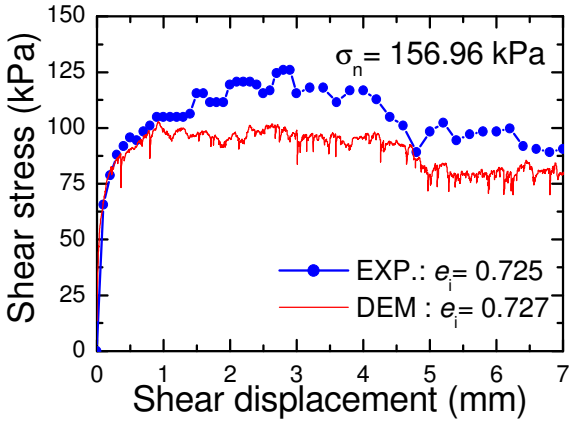

(a) Shear stress vs. shear displacement

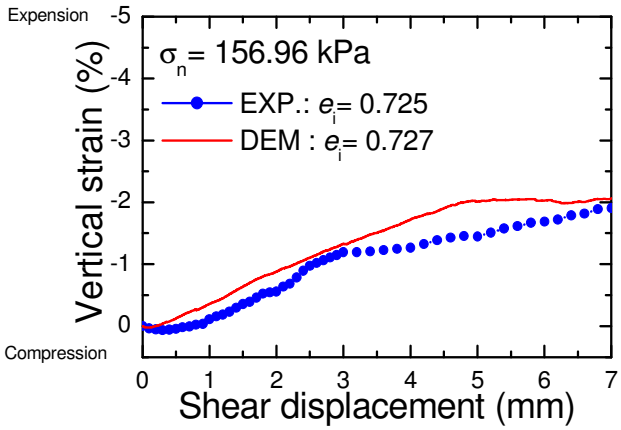

(b) Vertical strain vs. shear displacement

Figure 8 Example of comparison between direct shear tests and its DEM analysis results in case of 156.96 kPa in normal stress

Figure 9 shows the relationship between normal stress and shear strength including peak shear strength and residual shear strength in experiment comparing with its DEM results. The residual shear stresses in both the experiment and DEM simulation were defined by the value of shear stress at the shear displacement of 7 mm.

The results show that the shear strength in each normal stress obtained from DEM was smaller than the experimental results for peak state. In contrast, the DEM simulations showed good agreements with the experimental results in residual state.

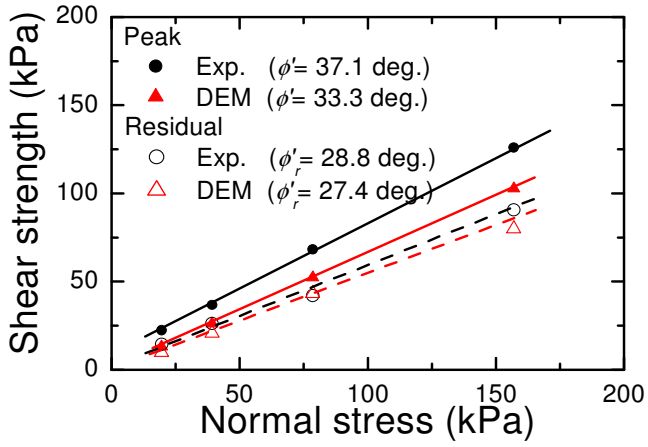

Fig. 9 Normal stress versus shear strength

It can be noted that the internal friction angle (33.3 deg.) calculated from DEM was greater than the friction angle between the balls (15 deg.). This is due to the fact that the internal friction angle is the friction angle of soil specimen (assembly of balls), which depends on the packing state of the specimen and dilatancy behaviour. Meanwhile, the friction angle between balls does not depend on the packing state of the specimen and dilatancy behaviour.

Based on the comparisons between the element tests and its DEM simulations, it can be judged that $k_n = 8\times10^6$ N/m = $4k_s$ is an appropriate spring stiffness which will be employed in DEM simulations of the push-up load tests of soil plugs.

4. PUSH-UP LOAD TESTS OF SOIL PLUGS; EXPERIMENT AND DEM ANALYSIS

4.1 Experimental Study Using Alumina Balls

The push-up load tests of the uncrushable soil plugs of the alumina balls were carried out in dense packing state (D_r greater than 90% or void ratio, e, less than 0.730). The ratio of height of soil plug to inner pile diameter, H/D, was varied from 3 to 6.

Figure 10 shows an illustration and photo of the push-up load test device used in this study. The test device consists of oil jack, load cell, dial gauge, rigid loading plate and model steel pipe pile. The properties of the model steel pipe pile have been listed in Table 2.

Figure 11 shows the arrangement of strain gauges instrumented on outer surface of the model pile. Twenty strain gauges were adhered on left and right sides of the pile at 10 levels for measurement of axial strains along the pile. Axial forces along the pile and shear forces acting on the inner shaft were calculated using measured strain distributions.

First, the model pipe pile with a rigid loading plate inside its bottom was set up. The load cell was placed between the oil jack and the loading plate for measurement of the push-up force, F. Then, the alumina balls were poured into inside the pipe pile from the pipe head by layer. In order to control the specified initial conditions of plug such as the aspect ratio, H/D, and the packing state, the pile was lightly hit with a rubber hammer. Finally, the dial gauge was set up at the bottom plate to measure the push-up displacement, S. The push-up force was applied using the oil jack with push-up displacement rate at 0.1 to 0.3 mm/s.

The initial properties of uncrushable plug in each push-up load test are summarised in Table 4. The void ratio of the plug in each test almost equals 0.7. The void ratio of the plug in each test was slightly smaller than the minimum void ratio of the alumina balls. This may be due to that the ratio of the inner pile diameter to the alumina ball diameter is greater than the ratio of the cylinder box diameter used in the maximum dry density test to the alumina ball diameter.

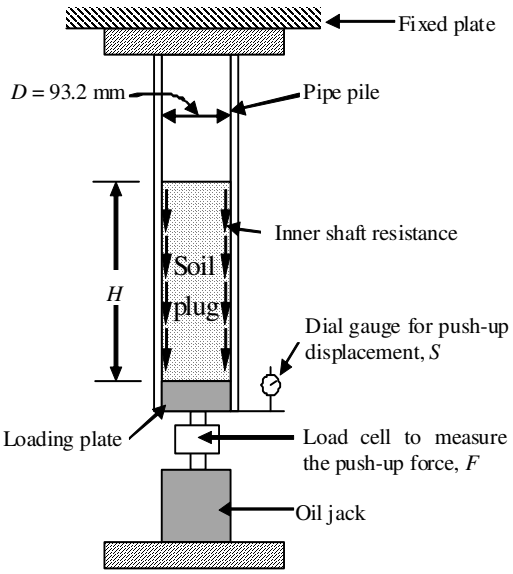

(a) Illustration of push-up load test device

(b) Test set-up

Fig. 10 Push-up load test device used in experimental study

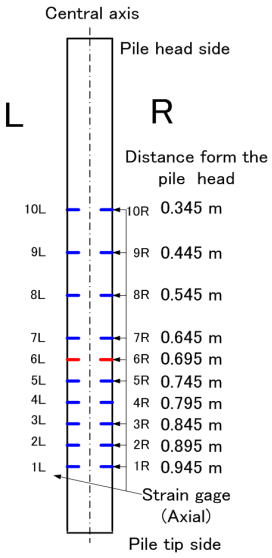

Fig. 11 Locations of strain gauges in the model pile

Table 4 Initial conditions of plugs using uncrushable particles

H/D	**3.0**	**3.5**	**4.0**	**4.5**	**5.0**	**5.5**	**6.0**
ρ_d (t/m^3)	2.153	2.154	2.156	2.161	2.157	2.178	2.201
e	0.709	0.708	0.707	0.703	0.706	0.689	0.672

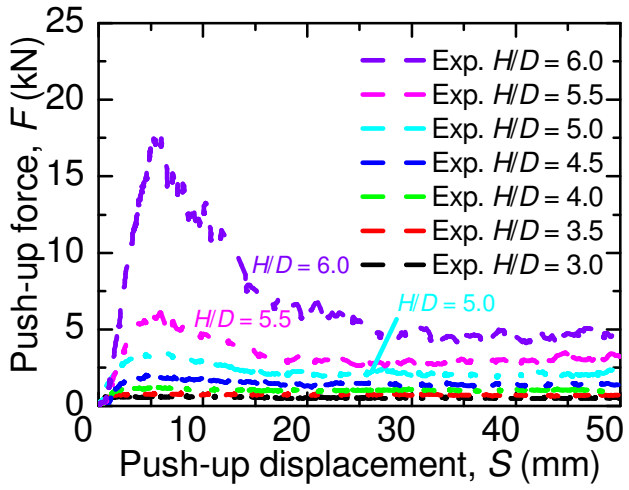

Figure 12 Relationship between push-up displacement and push-up force of the push-up load tests using uncrushable particles

Figure 12 shows the relationship between push-up displacement and push-up force in each H/D ratio. It was observed that peak push-up force occurred in all the tests. The peak push-up force increased with increase of H/D ratio. In early loading stages, the push-up forces rapidly increased and showed peak push-up force. After that, the push-up forces decreased gradually with increasing push-up displacement and levelled off when push-up displacements exceeded one-third of the inner pile diameter.

Let us see here the results of the push-up load tests for the cases of H/D = 4 and 6 in detail. Figure 13 shows the distributions of shear stresses acting along the inner pile shaft at each push-up displacement. The results indicate that the shear stresses increase exponentially from the top of the soil plug to the bottom. Very large shear stress was found in the vicinity of the bottom of soil plug. Hence, it is noted that lower part of soil plug especially adjacent to pile tip mainly resisted against the push-up force.

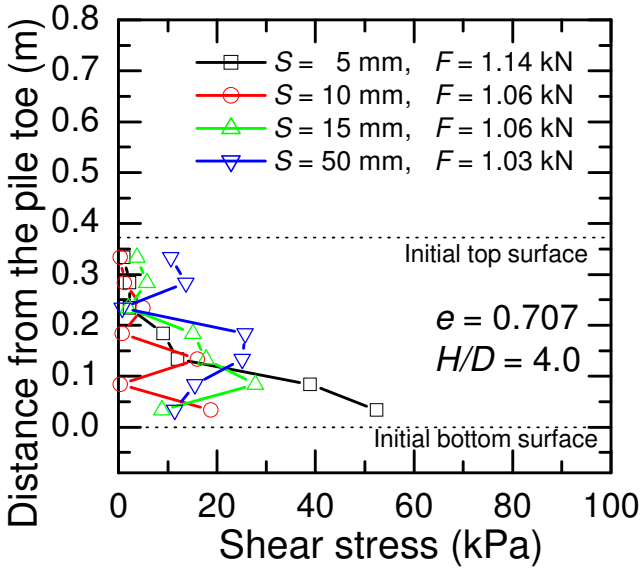

a) H/D = 4.0

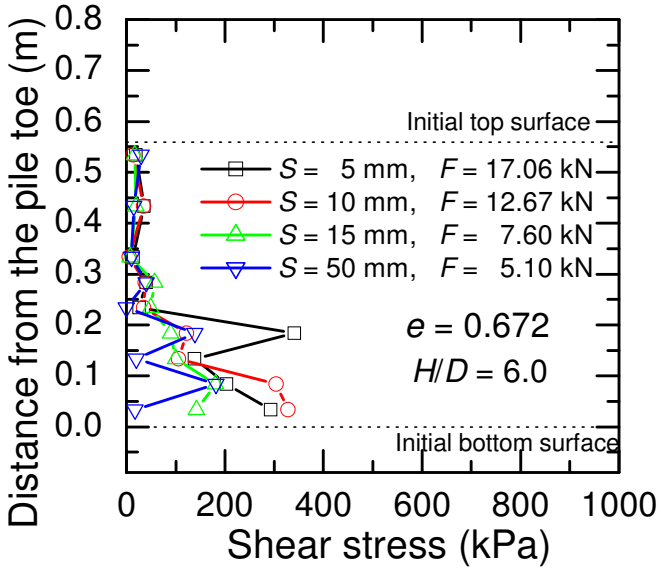

b) H/D = 6.0

Fig. 13 Example of distribution of shear stresses along inner pile shaft in each push-up displacement

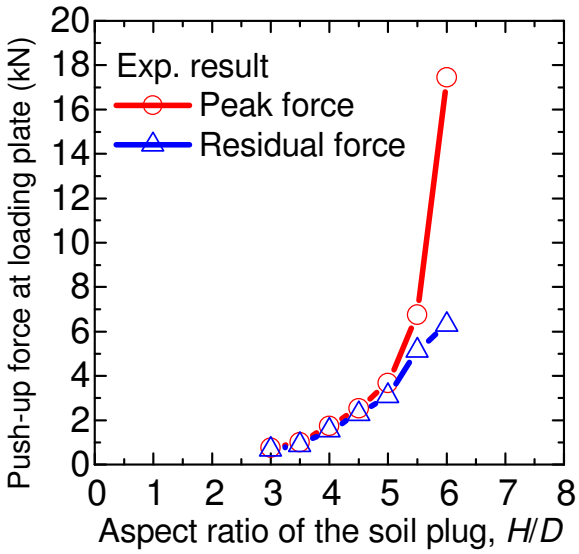

Fig. 14 Relationship between aspect ratio and push-up force

Figure 14 shows the relationship between H/D and push-up force. Residual force was the push-up force at a push-up displacement of 50 mm (approximately 50% of inner pile diameter). The results show that discrepancy between the peak force and the residual force starts to occur when H/D ratio exceeds 4.5. The discrepancy becomes greater as H/D ratio increases. A cause of the discrepancy between peak force and the residual force will be clarified through the numerical study on the push-up load tests.

As the results of the experiments using the alumina balls, no deformation and crushing of the alumina balls were not observed after the one-dimensional compression tests, direct shear tests and push-up load tests. These results confirm that the alumina balls used in the experiments can be treated as uncrushable particles.

4.2 DEM Analysis of the Push-up Load Tests

DEM simulations of the push-up load tests of uncrushable plugs in dense state with different aspect ratios, H/D, were carried out using the determined analysis parameters.

Table 5 shows the analysis parameters of spherical balls used in these DEM simulations. Friction coefficient between the balls was set at 0.268 (15 deg. in friction angle) that was obtained from the friction tests of the alumina balls by means of the inclined plane method in Fig. 4. The values of $k_n = 8\times10^6$ N/m = $4k_s$ were employed throughout these DEM simulations.

Table 5 Analysis parameters of spherical balls used in DEM simulations of push-up load tests

Property	value
Diameter of ball	4.0 mm
Density of ball particles, ρ_s	3.68 t/m^3
Friction coefficient (friction angle)between alumina balls	0.27 (15 deg.)
Normal spring stiffness, k_n	8×10^6N/m
Tangential spring stiffness, k_s	k_n /4

Figure 15 shows an analysis model of the push-up load tests of uncrushable soil plug. The soil plug was modelled as assembly of the spherical balls. The aspect ratio of soil plug, H/D, was set at 3.0, 4.0, 5.0 and 6.0, which corresponded to the experimental conditions. The initial void ratio of the soil plug prior to push-up loading was set at 0.700.

The model pipe pile was modelled by rigid walls. Hence, the deformation of the pile was not taken into account in this analysis. Table 6 summarises the analysis parameters of the model pile used.

The value of spring stiffness between the wall and the ball were kept the same as the values of the spring stiffness between the spherical balls. The friction coefficient between the spherical ball and the wall was set at 0.35 that obtained from the shear tests between the alumina ball and inner pile shaft surface of the model pile (see Fig. 2).

In process of DEM simulation in each H/D, the spherical balls were generated inside the model pipe pile to form plug. Then, self-weight analysis was conducted without the friction between ball and the inner pile surface. Finally, the simulation of push-up load test was carried out with the friction between ball and the inner pile surface by applying an upward velocity of 5 mm/s at the bottom plate. Throughout the simulation, the forces acting on each rigid wall were calculated.

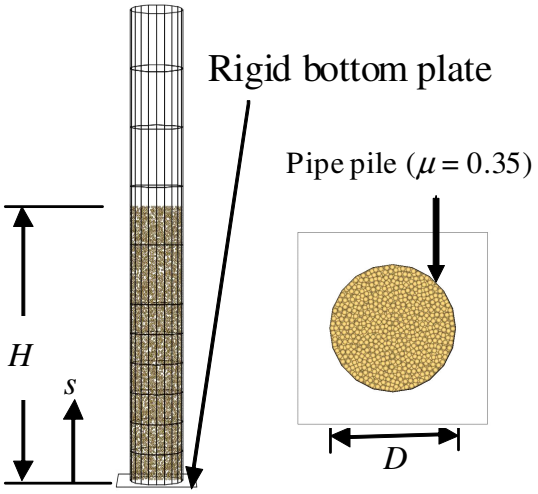

Fig. 15 Analysis models of the push-up load tests

Table 6 Analysis parameters of model pile

Property	value
Diameter	93.2 mm
Length	800 mm
Friction coefficient (friction angle) between alumina ball and inner pile surface	0.35 (19.3 deg.)
Normal spring stiffness, k_n	8×10^6 N/m
Tangential spring stiffness, k_s	k_n/4

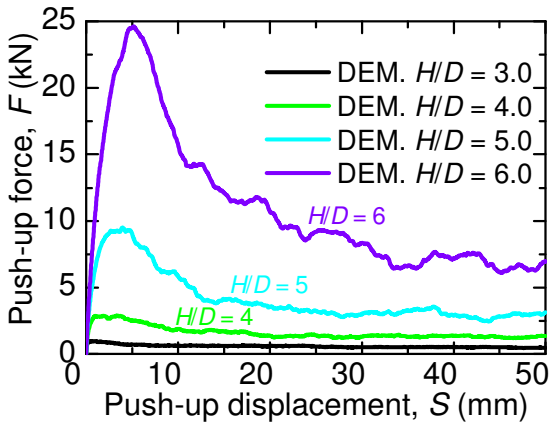

Fig. 16 Push-up displacement vs. push-up force in DEM

Figure 16 shows the relationship between push-up force and push-up displacement for 4 cases of the simulations in which H/D = 3.0, 4.0 5.0 and 6.0. The DEM results show that hardening and softening behaviours occur in all the cases. The push-up forces increase shapely in early loading stage and show the peak push-up forces. Then, the push-up forces decrease rapidly and level off when the push-up displacements exceed one-third of the pile diameter. The peak push-up force increases with increase of H/D.

Figure 17 shows the comparison between the experimental and DEM results in case of H/D = 6.0. The tendency obtained from the DEM simulation is totally similar to the experimental result. However, the magnitude of peak push-up force in DEM is greater than the experimental value to a considerable degree. This seems to be attributed to the fact that the resistance due to the dilation of plugs in DEM is greater than in the experiment because the model pile in DEM was modelled as perfectly rigid body, whereas the model pile used in the experiments was not rigid when comparing the stiffness of the model pile with the stiffness of the alumina balls. Consequently, the larger radial force (stress) resulting in larger shear force (stress) and larger push-up force are obtained in DEM compared with the experimental results.

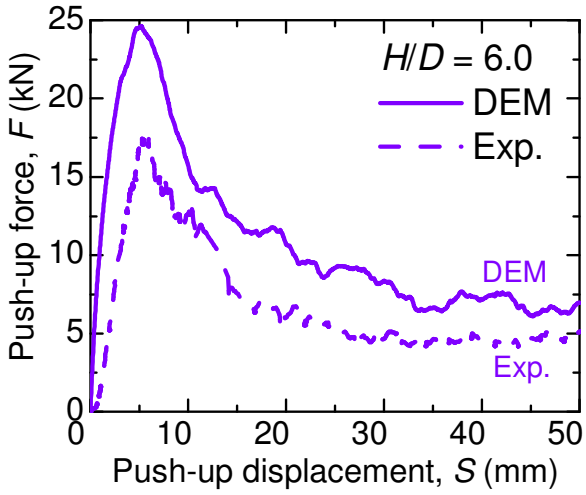

Fig. 17 Comparison between the experimental and DEM results in case of H/D = 6.0

Let us see here the results of the DEM simulations for the cases of H/D = 4.0 and 6.0 in detail. Figure 18 shows the inner shear stress distribution along the model pile. The shear stresses increase exponentially from the top to the bottom of the soil plug. Very large shear stresses are mobilised along the vicinity of the bottom of soil plug. This result clearly indicates that lower portion of soil plug mainly resists the push-up force. Similar results were obtained in the other DEM simulation cases.

The above-mentioned DEM results simulate approximately the experimental results (Fig. 13) qualitatively. However, the magnitudes of mobilised shear stress in DEM especially at the bottom portion of the soil plug are greater than the experiment.

In addtion to the above-mentioned factor that can affect the stress distribution, it should be noted here that the inner shear stress distributions in Fig. 13 were calculated from the measured axial strains of the model pile with an assumption that the influence of radial stresses acting on the inner pile surface on axial strains is negligible. That is, axial forces of the pile were calculated as the measured axial strain multiplied by Young's modulus and the cross-sectional area of the pipe pile. The inner shear stress between two levels of strain measurements of the pile was calculated as the difference of the axial forces at the two levels devided by the corresponding inner surface area.

Although the authors are aware that this procedure is valid only when radial stresses are small enough, there was no other choice in our experimental set-up.

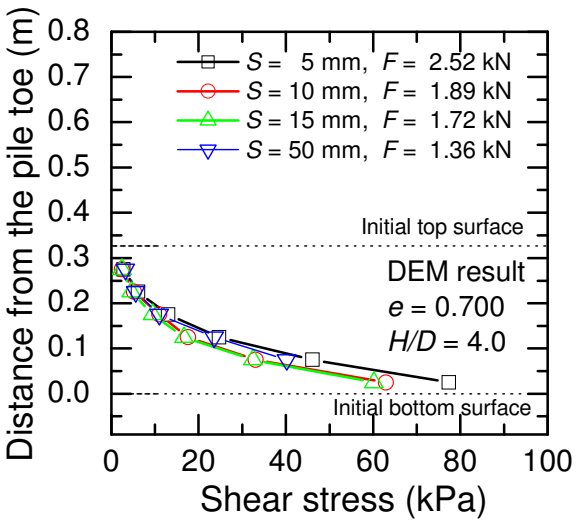

a) H/D = 4.0

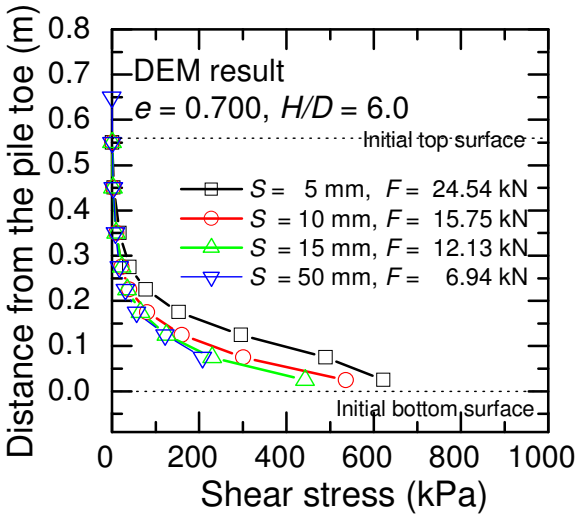

b) H/D = 6.0

Fig. 18 Distribution of shear stress along inner pile shaft

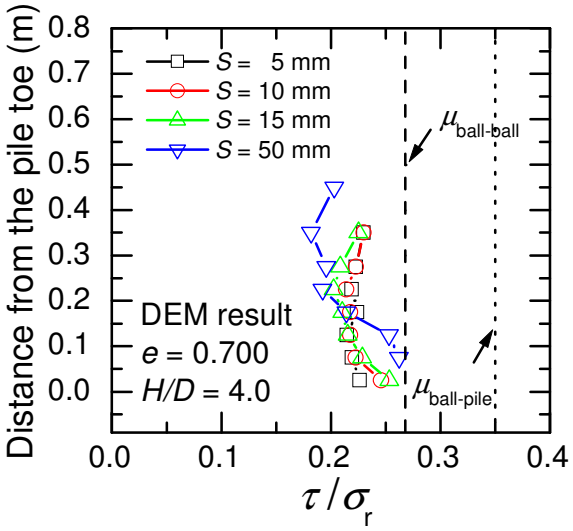

a) H/D = 4.0

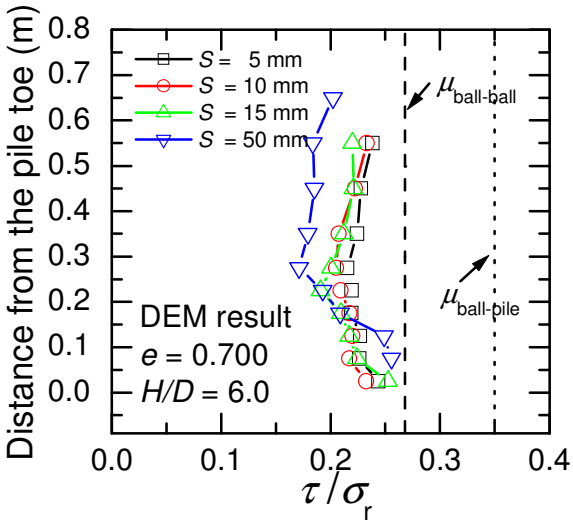

b) H/D = 6.0

Fig. 19 Distribution of friction coefficient along inner pile shaft

Figure 19 shows the distribution of mobilised friction coefficient along the model pile in cases of H/D = 4.0 and 6.0. The friction coefficient along the inner pile shaft was calculated from the ratio of the mobilised shear stress, □, to the radial stress, □$_r$, acting on the inner pile shaft. The dashed line in each figure represents the friction coefficient between the alumina balls (= 0.268), while the dotted line in each figure represents the friction coefficient between the alumina ball and the inner pile shaft (= 0.350), which were used in the DEM analyses. Note that internal friction coefficient of the alumina balls obtained from DEM analysis of the direct shear test is 0.65 (see Fig. 9).

During push-up loading, the mobilised soil-pile friction coefficient at the bottom portion of the soil plugs increases a bit and is found as a maximum friction coefficient. Meanwhile the mobilised soil-pile friction coefficient at middle and top of the soil plug decreases with increasing push-up displacement and reaches to 0.18. Peak push-up force was mobilised at push-up displacement of around 5 mm in the experiments (Fig. 12) and the DEM analyses (Fig. 16). It can be seen from the DEM analyses that after the peak push-up force is reached, the mobilised friction coefficient along the middle and upper portions of the soil plug decreases and the mobilised friction coefficient along the bottom of the soil plug increases, resulting in overall reduction of the push-up force. This trend is remarkable in case of H/D = 6 (Fig. 19). This behaviour could explain the experimental results shown in Fig. 14.

Furthermore, it is noticeable that the maximum of soil-pile friction coefficient obtained from the DEM analysis does not exceed the friction coefficient between the alumina balls (dashed line) that is smaller than the soil-pile friction coefficient. So, the smaller value of either particle-to-particle friction coefficient or particle-to-pile friction coefficient controls the soil plug capacity.

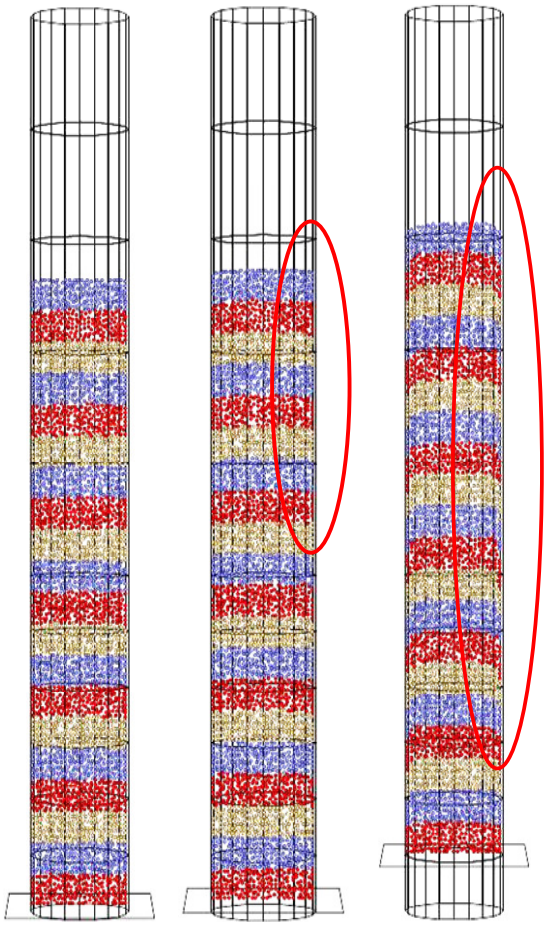

a) S = 5 mm Peak state | b) S = 15 mm After peak force | c) S = 50 mm Residual state

Fig. 20 Movements of spherical balls inside the pile during push-up loading in case of H/D = 6.0

It is also noted that mobilised friction coefficient is smaller than particle-to-particle friction coefficient, suggesting that rotation of particles also controls the plug capacity.

Figure 20 shows movements of spherical balls inside the model pile at 3 push-up displacements. Figures 20(a), (b) and (c) show the movements of the soil particles at the peak push-up force (at S = 5 mm), after the peak push-up force (at S = 15 mm), and the residual state (at S = 50 mm), respectively.

The results showed that the plug in any locations was compressed until the peak force, which corresponded to a very small movement of particles in any location. After the peak force, the particles at the upper portion of the soil plug started to move upward, resulting to the upper portion of the soil plug becomes looser. During post-peak loading, degree of the particle movement increased and progressed to middle and lower portion of the soil plug as the push-up displacement increases and the soil plug finally reaches the residual state (Fig. 20(c)). It can be judged that the loosening behaviour progresses to middle and lower portions of the soil plug. Meanwhile the lower portion of the plug up to 1D from the bottom continues to be compressed and becomes denser as the push-up displacement increases.

This behaviour corresponds to the decrease of the mobilised friction coefficient in upper portion of the soil plug and the increase of mobilised friction coefficient in lower portion of the soil plug (Fig. 19).

Figure 20(c) clearly indicates convex deformations at the middle and upper portions of the soil plug resulted from larger movements of the soil particles at the centre of the pile. Although it is difficult to show in the paper using figure, it was shown from close observation of the calculated results that the shear failure occurs inside the soil plug with large degree of rotation of particles close to the inner pile surface, which may result in the decrease of the mobilised friction coefficient except for the bottom portion.

5. COMPARISON WITH PUSH-UP LOAD TESTS OF SOIL PLUGS USING SILICA SAND

5.1 Push-up Load Tests of Silica Sand Plug

The push-up load tests of crushable soil plugs were carried out. Dry silica sand was used as the crushable soil particles to form the soil plug within the same model steel pile.

The physical properties of the silica sand were obtained from the element tests including particle density test, maximum and minimum dry density tests, one-dimensional compression test, direct shear test and shear test between the silica sand and the model pile without rotation of the soil particles. The physical properties of the silica sand are summarised in Table 7. The properties of the model steel pipe pile are listed Table 8.

Table 7 Physical properties of the crushable silica sand

Property	Value
Density of soil particle, ρ_s	2.68 t/m^3
Maximum dry density, $\rho_{d\,max}$	1.69 t/m^3
Minimum dry density, $\rho_{d\,min}$	1.39 t/m^3
Maximum void ratio, e_{max}	0.927
Minimum void ratio, e_{min}	0.583
Mean grain size, D_{50}	0.126 mm
Coefficient of uniformity, U_c	2.27

Table 8 Properties of the model pipe pile

Property	Value
Young's modulus	201 GPa
Length	1.1 m
Inner diameter	93.2 mm
Outer diameter	101.4 mm
Friction coefficient (friction angle) between inner pile shaft and silica sand	0.50 (26.6 deg.)

The test device and test procedure were kept the same as the push-up load tests of the uncrushable soil plug (alumina balls) in order to compare the results between the uncrushable (alumina ball) and crushable soil plug (silica sand). Illustration and photo of the push-up load test device have been indicated in Fig. 10. The model steel pipe pile used in this test was the same as that used in the tests of uncrushable plugs (see Fig. 11).

The push-up load tests of the dry silica sand plugs were carried out in loose state (D_r = 50 to 60%), medium state (D_r = 70 to 80%) and dense state (D_r> 90%). The aspect ratio, H/D, was varied from 3 to 5 in each packing state.

Figure 21 shows the relationship between push-up force and push-up displacement in cases of loose, medium and dense packing states. The experimental results indicated that the push-up force increases with increase of H/D as well as the initial packing state of soil plug. The push-up force continued to increase with increase of the push-up displacement without showing softening behaviour in all cases. It is noted that two different shapes of the force-displacement relation were observed only in the dense packing state. It seems that there is a critical aspect ratio $(H/D)_{crit}$ which separates the two different shapes of that relation.

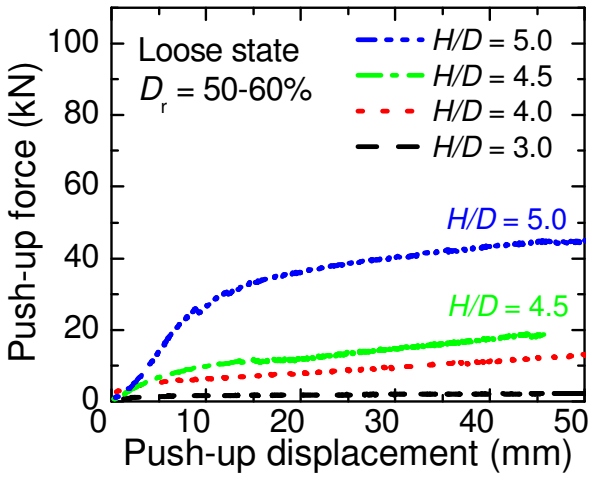

(a) Loose packing state

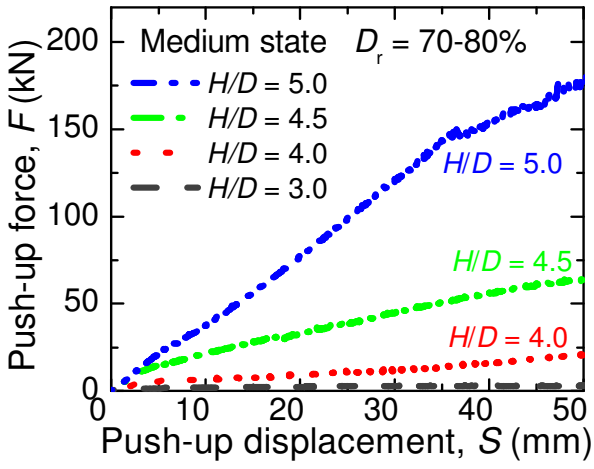

(b) Medium packing state

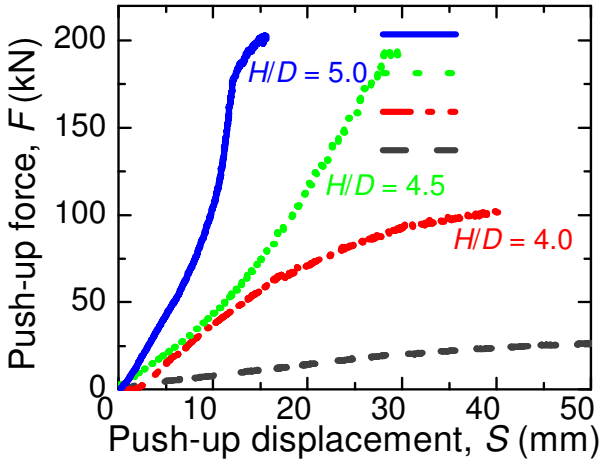

(c) Dense packing state

Fig. 21 Results of push-up load tests of sand plugs

Figure 22 shows distribution of mobilised shear stress along the pile in case of H/D = 4 and 5 of the dense sand plug. The results conformed with the results obtained in the push-up load tests of the alumina balls qualitatively, in which very large shear stress was found along the vicinity of the bottom of sand plug.These results insisted that bottom portion of soil plug mainly resists against the push-up force.

After each push-up load test, sieve analysis of the silica sand was conducted. The sand plug was roughly divided into upper portion and lower portion.

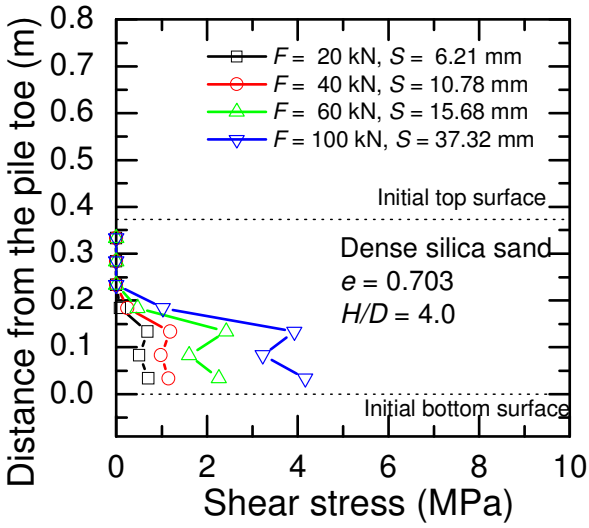

a) H/D = 4.0

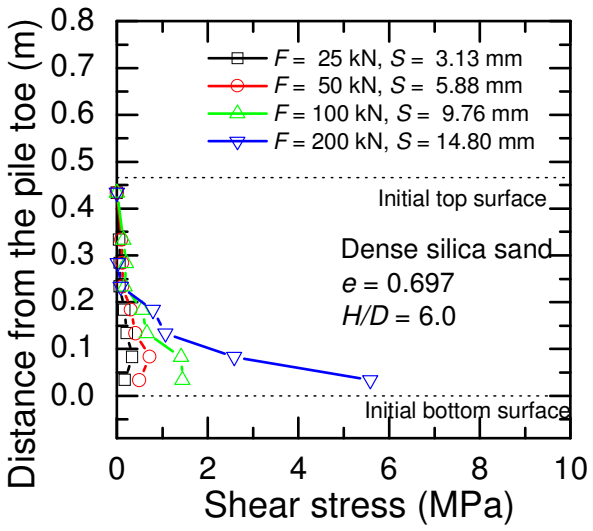

b) H/D = 5.0

Fig. 22 Example of distribution of shear stresses along inner pile shaft in case of the silica sand

Figure 23 shows the sieve analysis results of the upper and lower portions of sand plug after the test of medium sand plug having H/D = 5 with the original grain size distribution of the silica sand. The sieve analysis results showed that passing percentages of sand particles finer than 0.4 mm after the push-up load test were slightly higher than its original size distribution.

In addition, close inspection of the sieve analyses also indicated that the sand from the lower portion of the sand plug had larger amount of fine components than the upper portion of the sand plug, although the difference was very small. This result suggested that the crushing of soil particles occurs during push-up loading especially in the lower portion of the soil plug.

In order to reaffirm the particle crushing phenomenon, oedometer tests of loose, medium and dense sand specimens were carried out to high vertical stress level, together with conducting sieve analyses of the soil specimens after the oedometer tests.

Figure 24 shows the results of the oedometer tests. The results are shown in term of effective vertical stress, p, versus void ratio, e. The yield stress was observed clearly in each packing state. The yield stresses were estimated as 2000 kPa, 1600 kPa and 1500 kPa for loose, medium and dense specimens, respectively. The average yield stress was estimated as 1700 kPa. The compressibility in each specimen increased rapidly when vertical stress exceeded the yield stress.

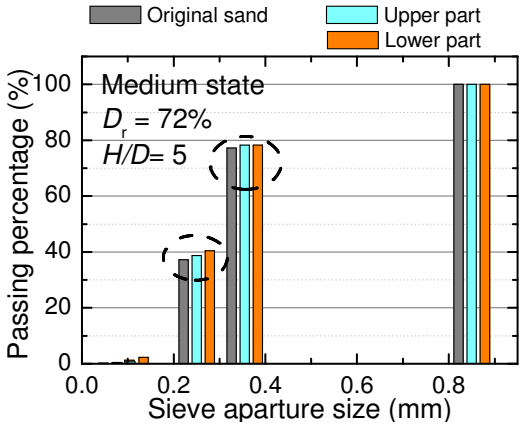

Fig. 23 Comparisons of sieve analysis results of the upper and lower portions of sand plug after the push-up load test, together with grain size distribution of the original sand

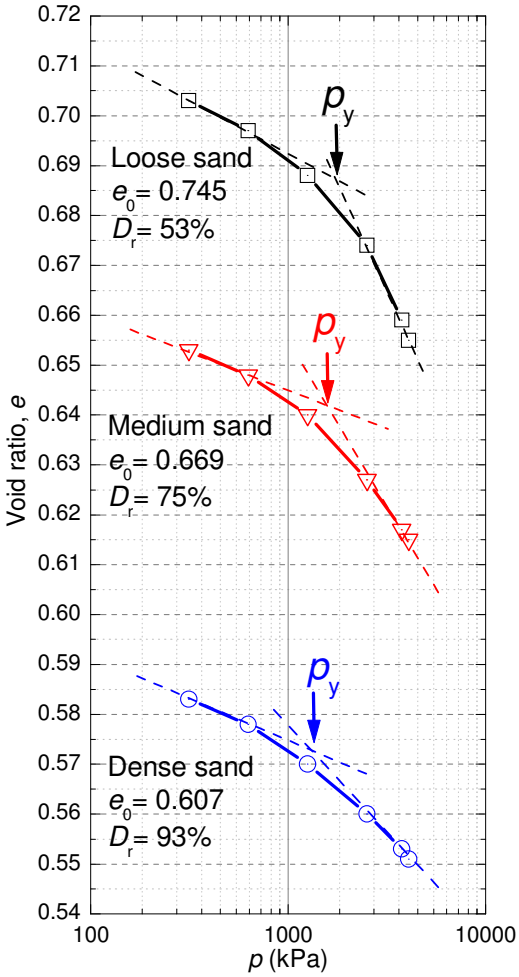

Fig. 24 Results of oedometer tests of loose, medium and dense sand specimens

Figure 25 shows the results of the sieve analyses of the sand specimens after the oedometer tests in which the vertical stress, p, reached 4080 kPa. The results clearly showed that passing percentages of the sand particles finer than 0.4 mm after the oedometer tests were greater than the original distribution in all cases, indicating clearly that the particle crushing occurred. High degree of particle crushing was observed in the loose specimen compared with the medium and dense specimens. The results indicate that large amount of particle crushing would have occurred after vertical stress exceeded the yield stress.

So in the push-up load tests of the dry silica sand plugs, push-up force of 11.6 kN corresponded to the vertical stress at the bottom of the sand plug of 1700 kPa that is the average yield stress of loose, medium and dense specimens. This value is recognised as a threshold value where the particle crushing starts to occur.

Therefore, these results suggested that particle crushing in the dry silica sand plug may have occurred in several cases of the push- up load tests, because the push-up forces exceed this threshold value.

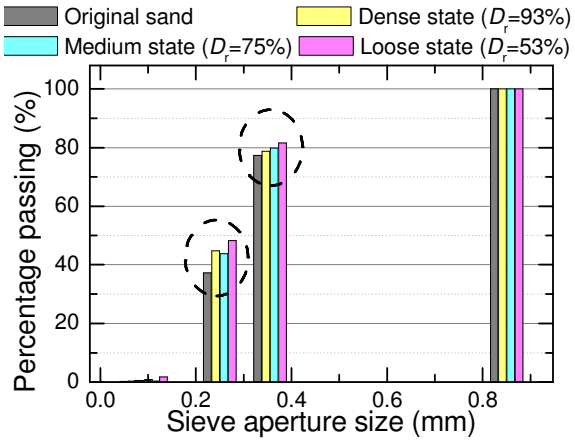

Figure 25 Results of sieve analyses after the oedometer tests comparing with grain size distribution of the original sand

5.2 Comparison of the Two Experimental Results

The push-up load tests of soil plugs using the alumina balls and the silica sand have been carried out using the same test device and test procedure. The detailed results of the two tests have been described above.

Based on the load-displacement relation, the results of the push-up load tests of the alumina ball plugs (see Fig. 12) and the silica sand plugs (see Fig. 21) indicated the same result that the maximum push-up force increases with the increase of H/D ratio. However, two different patterns of the relation between the two experimental results have been clearly observed.

In case of the alumina balls, the push-up force increased rapidly and showed the peak value. After the peak, the force showed a subsequent drop to residual value. The residual value of the push-up force increased with increasing H/D. Hardening and softening behaviours were clearly observed in all cases.

In contrast, the push-up force in a given H/D ratio obtained from the push-up load tests of the silica sand plugs increases continuously with the increase of push-up displacement. Softening behaviour was not observed in all cases. For close inspection of the test results of the dense silica sand plugs, a critical aspect ratio $(H/D)_{crit}$ that separates two different shapes of load-displacement relation was found between H/D = 4.5 and 5.0. When H/D is greater than $(H/D)_{crit}$, the push-up force can be developed rapidly with small push-up displacement. In contrast for H/D less than $(H/D)_{crit}$, the push-up force increases gradually when push-up displacement increases.

Although the test device and procedure were kept the same in the both experiments except for the crushability of the model soil particle, it was difficult to identify that the crushability of the soil particle is the significant parameter influencing on the different patterns of the load-displacement relations between the two experimental results, because the particle size distribution and particle shape between the two model soils were different. However, it can be judged that the crushability of soil particles is one of possible parameters influencing on the soil plug behaviour.

6. CONCLUSIONS

In this study, push-up load tests of soil plugs in a steel pipe pile and its DEM analyses have been carried out. Uncrushable uniform spherical particles (alumina balls) were used to model the soil plugs. Element tests of alumina balls and its DEM analyses such as one-dimensional compression tests and direct shear tests were carried out at the beginning to characterise the alumina ball and determine the suitable DEM parameters. Then, the push-up load tests and its DEM simulations were carried out.

Thereafter, the experimental results were compared with the results of push-up load tests of the silica sand plugs using the same test device and test procedure.

Main findings from the experimental study are summarised as:

1) Two different patterns of the soil plug behaviour were observed. That is, in the experiment using the alumina balls the load-displacement relation showed a peak push-up force and a subsequent drop to residual value in all cases, whereas the load-displacement relation in the tests using the silica sand showed monotonic increase in the push-up load. It is inferred that the crushability of soil particles is one of parameters influencing on overall soil plug behaviour in addition to the particle size distribution and the shape of particles.
2) For the silica sand plugs, a critical aspect ratio $(H/D)_{crit}$ that separates two different shapes of load-displacement relation was found in dense state only. When H/D is greater than $(H/D)_{crit}$, the push-up force can be developed rapidly with small push-up displacement. In contrast, for H/D less than H/D_{crit}, the push-up force increases gradually when push-up displacement increases.

Beneficial conclusions and suggestions from the numerical study are as follows:

1) The maximum soil-pile friction coefficient is mobilised at the bottom portion of soil plug due to the large shear stresses at the bottom portion. The maximum mobilised soil-pile friction is less than the prescribed soil-pile friction, suggesting that rotation of particles occurs adjacent to the soil-pile interface, and controls the plug capacity.
2) The movements of soil particles showed that the soil plug Qin any portion is compressed and becomes denser until the peak force. After the peak force to the residual force, the upper portion of the soil plug becomes looser. The loosening behaviour progresses from the upper to the middle and lower portions of the soil plug as the push-up displacement increases. Meanwhile the bottom of the soil plug continues to be compressed and becomes denser.
3) Based on the good agreements between the experiments and its DEM analyses of the push-up load tests, matching analysis between the element tests and its DEM simulations is one of practical approaches for estimating the DEM analysis parameters.

This paper carried out the push-up load tests of soil plug and its DEM analysed using uniform spherical balls with a relatively large size. Essentially, soil consists of various sizes of soil particle and the size of soil particle is very small compared with the size of particles used this study.

Further study, investigation on influences of particle size and particle size distribution on the plugging behaviour using experiment and DEM will be necessary

7. ACKNOWLEDGEMENTS

The authors would like to express our gratitude to Assoc. Prof. Kenichi Maeda, Nagoya Institute of Technology, for his helpful suggestions in the numerical study. We wish to thank also Mr. Shinya Shimono and Mr. Hiroyoshi Murota, Kanazawa University, for their supports in the experimental study.

8. REFERENCES

Byrne, B.W. (1995): Driven pipe piles in dense sand, Australian Geomechanics, 27, Paper No. 9501, pp.72-80.

De Nicola, A. and Randolph, M.F. (1997): The plugging behaviour of driven and jacked piles in sand, Géotechnique, 47(4), pp841-856.

Gavin, k. g. and lehane, b.m. (2003): The shaft capacity of pipe piles in sand, Canadian Geotechnical Journal, 40, pp.36-45.

Hight, D.W., Lawrence, D.M. Farquhar, G.B., Milligan, G.W.E., Gue, S.S. and Potts, D.M. (1996): Evidence for scale effects in the end bearing capacity of open-ended piles in sand. Proceeding of 28th Offshore Technology Conference, Texas, pp.181-192.

Itasca (2003): PFC3D Manual, Itasca Consulting Group, USA.

Kanno, T., Yamakawa, S., Onishi, M. and Miura, H. (1978): Blockade sand effect of large diameter open-ended pipe piles. Technical report of Sumitomo Metal Industries, 30(1), pp.52-61 (in Japanese).

Katzenbach, R. and Schmitt, A. (2004): Micromechanical modelling of granular materials under triaxial and oedometric loading, Proceedings of 2nd International PFC Symposium, Kyoto, pp.313-322.

Kishida, H. and Isemoto, N. (1977): Behaviour of sand plugs in open-ended steel pipe piles, Proceedings of 9th International conference on soil mechanism, Tokyo, 1, pp.601-604.

Kitiyodom, P., Matsumoto, T., Hayashi, M., Kawabata, N., Hashimoto, O., Ohtsuki, M. and Noji, M. (2004): Experiment on soil plugging of driven open-ended steel pipe piles in sand and its analysis, Proceedings of 7th International Conference on the Application of Stress-Wave Theory to Piles, Selangor, pp.447-458.

Leong, E.C. and Randolph, M.F. (1991): Finite element analyses of soil plug response, International Journal for Numerical and Analytical Methods in Geomechanics, 15, pp.121-141.

Liyanapathirana, deeks, a.j. and randolph, m.f. (1998): Numerical analysis of soil plug behaviour inside open-ended pipe piles during driving, International Journal for Numerical and Analytical Methods in Geomechanics, 22, pp. 303-322.

Liyanapathirana, deeks, a.j. and randolph, m.f. (1998): Numerical modelling of large deformations associated with driving of open-ended piles, International Journal for Numerical and Analytical Methods in Geomechanics, 24, pp. 1079-1101.

Liyanapathirana, deeks, a.j. and randolph, m.f. (2001): Numerical modelling of the driving response of thin-walled open-ended piles, International Journal for Numerical and Analytical Methods in Geomechanics, 25, pp. 933-953.

Matsumoto, T. and Takei, M.(1991): Effect of soil plug on behaviour of driven pipe pile, Soil and Foundation, 31(2), pp.14-34.

Matsumoto, T., Michi, Y. AND Hirano, T. (1995): Performance of axially loaded steel pipe piles driven in soft rock, Journal of Geotechnical Engineering, ASCE,121(4), pp.305-315.

Matsumoto, T., Kitiyodom, P., Wakisaka, T. and Nishimura, S. (2004): Research on plugging of open-ended steel pipe piles and practice in Japan, Proceedings of 7th International Conference on the Application of Stress-Wave Theory to Piles, Selangor, pp.133-152.

Ovesen, N.K. (1979): The scaling law relationship - Panel Discussion, Proceedings of 7th European Conference on Soil Mechanics and Foundation Engineering, Vol.4, pp.319-323.

Paik, K.H., and Salgado, R. (2003): Determination of bearing capacity of open-ended piles in sand, Journal for Geotechnical and Geoenvironmental Engineering, 129(1), pp. 46-57.

Paik, K.H., Salgado, R., Lee, J.H. and Kim, B.J. (2003): The behaviour of open- and closed-ended piles driven into sands, Journal for Geotechnical and Geoenvironmental Engineering, 129(4), pp. 296-306.

Paikowsky, S.G. and Whitman, R.V. (1990): The effects of plugging on pile performance and design, Canadian Geotechnical Journal, 27, pp 429-440.

Randolph, M.F., Leong, E.C. and Houlsby, G.T. (1991): One-dimensional analysis of soil plugs in pipe piles, Géotechnique, 41(4), pp. 587-598.

Randolph, M.F., May, M., Leong, E.C., Hyden, A.M. and Murff, J.D. (1992): Soil plug response in open-ended pipe piles, Journal of Geotechnical Engineering, ASCE, 118(5): pp.743-759.

Thongmunee, S., Kobayashi, S., and Matsumoto, T. (2010): DEM simulations of push-up load tests of sand plug in steel pipe pile, International Symposium on Geomechanics and Geotechnics: From Micro to Macro (IS-Shanghai 2010), pp. 721-726.

Yamahara, H. (1964a): Plugging effects and bearing mechanism of steel pipe piles (Part 1), Transaction of the Architectural Inst. of Japan, 96, pp. 27-37 (in Japanese).

Yamahara, H. (1964b): Plugging effects and bearing mechanism of steel pipe piles (Part 2), Transaction of the Architectural Inst. of Japan, 97, pp. 34-41 (in Japanese).